ELSEVIER

27 March 1998

Chemical Physics Letters 285 (1998) 410–416

CHEMICAL PHYSICS LETTERS

K_a-mixing in the unimolecular dissociation of NO_2 studied by classical dynamics calculations

S.Yu. Grebenshchikov [a], H. Flöthmann [a], R. Schinke [a], I. Bezel [b], C. Wittig [b], S. Kato [c]

[a] *Max-Planck Institut für Strömungsforschung, Bunsenstraße 10, D-37073 Göttingen, Germany*
[b] *Department of Chemistry, University of Southern California, Los Angeles, CA 90089, USA*
[c] *Department of Chemistry, Kyoto University, Sakyo-ku, Kyoto 606, Japan*

Received 23 December 1997

Abstract

Coriolis and centrifugal vibration–rotation coupling in the unimolecular dissociation of ground electronic state NO_2 has been examined by using classical trajectories. The time evolution of the projection K_a of the rotational angular momentum N in a body-fixed frame is analyzed. The main result is a relation between the decomposition lifetime and the degree of K_a-mixing. For example, less than 30% of the available K_a space becomes populated for an average lifetime of 5 ps. This is consistent with the conclusions, based on time-resolved experiments, that rotation–vibration transfer is slower than reaction except just above the threshold. © 1998 Elsevier Science B.V.

1. Introduction

The issue of intramolecular redistribution is central to the use of transition state theories to predict unimolecular reaction rates [1]. Namely, such theories are premised on the assumption of unbiased access to the phase space that includes all participating (coupled) degrees of freedom [1]. Implicit in this is that intramolecular redistribution is much faster than dissociation. Numerical studies have shown that this is usually true for vibrations of even triatomic molecules [1,2], provided that the modes are strongly coupled and the density of vibrational states is high. As a consequence of extensive experimental studies [3], progress in the field of nonlinear mechanics (see, for example, Ref. [4]), and computer experiments [5], transfer between *vibrational* degrees of freedom is now reasonably well understood both classically and quantum mechanically. Far less is known about excitation transfer between *vibrational* and *rotational* degrees of freedom (see, Refs. [6] and [7]).

Rotation increases the phase space volume by a factor of roughly $(2N + 1)$, where N is the quantum number for the rotational angular momentum, N. This increase is due to different orientations of N relative to a body-fixed axis. Were the rotational degrees of freedom decoupled from vibrations, this increase would have no effect on the reaction rate. However, vibration–rotation (VR) coupling is always present and its efficacy dictates which portions of the phase space participate in reaction [1]. Thus, one may anticipate a change of the dissociation rate with N.

For prolate symmetric tops ($I_a < I_b = I_c$), significant changes in rotational energy are associated with K_a, the projection of N on the body-fixed a-axis [8].

PII S0009-2614(98)00076-1

Of course, if K_a changes on the time scale of the experiment, it is obviously not a good quantum number. This is referred to as K_a-mixing.

The issue of K_a-mixing in the unimolecular dissociation of NO_2 has been examined in the early statistical treatments of the reaction [9]. Recently, the issue has been the focus of renewed attention, and conclusions have been drawn from different experiments carried out near reaction threshold, i.e. time-resolved pump-probe measurements [10] and spectroscopic studies [11,12]. For example, following the initial work of Miyawaki et al. [11], Abel et al. [12] examined product yield spectra and concluded that K_a-mixing is almost complete, whereas Ionov et al. [10], examined NO buildup times and concluded that K_a-mixing is incomplete. Note that the degree of K_a-mixing usually eludes direct experimental observation, though a few counter-examples exist [1]. Most frequently – and this applies to the experiments mentioned above – conclusions about K_a-mixing are based on indirect evidence such as counting lines in spectra of reactive resonances or statistical analyses of dissociation rates.

In this Letter, K_a-mixing brought about by Coriolis and centrifugal VR coupling is examined in NO_2 dissociation by using a global potential energy surface (PES) for the ground electronic state and classical mechanics for the dynamics. It is found that the extent of K_a-mixing is related to the decomposition rate. The results are consistent with both the time-resolved [10] and the spectroscopic studies [11,12], i.e. K_a-mixing is incomplete under the conditions of the former and nearly complete under the conditions of the latter.

2. Vibration–rotation coupling in NO_2

The spectroscopy and photodissociation of NO_2 have been studied extensively [13–21]. The optically accessible states of concern have mixed $^2A_1/^2B_2$ character due to coupling of the zeroth-order $^2A_1$ ground and $^2B_2$ excited states above their conical intersection [15,20]. Spectroscopic studies have confirmed that K_a-mixing is substantial just below the dissociation threshold D_0 [14,15,18].

When NO_2 is excited above D_0, the goodness (or lack thereof) of K_a as a quantum number becomes less obvious, mainly because the timescale over which VR coupling can induce K_a changes is limited to the unimolecular decomposition lifetime. In the time-resolved experiments [10] the dissociation rate has been measured as a function of N for average excess vibronic energies of 18 and 53 cm^{-1}. The corresponding spectral widths of the laser pulses were 30 and 100 cm^{-1}, respectively. In fitting the observed rates to RRKM models, the assumption of minimal K_a-mixing yielded the best agreement. This led the authors to conclude that K_a-mixing is incomplete. However, the most recent spectroscopic experiments [12] accessed the first 8 cm^{-1} above the threshold. A preliminary analysis of the line density indicated almost complete K_a-mixing, and fitting the observed resonance widths by using SACM provided further support that K_a-mixing is strong.

Both the spectroscopic and time-resolved measurements yield threshold rates, the former just above D_0 and the latter averaged over the laser linewidth. Theoretical modeling should be consistent with these observations. The present modeling is focused on the destruction of K_a as a good quantum number. Possible mechanisms are listed below.

(1) *Coriolis and centrifugal interactions* arise through dynamical distortions of the equilibrium molecular geometry. They are enhanced by large-amplitude motion in the highly vibrationally excited states which are involved in dissociation [13]. Matrix elements of the Coriolis interaction couple states with $\Delta K_a = \pm 1$, leaving N intact.

(2) *Spin-rotation interaction* was found to be the main source of rovibronic interaction when states with $J = 1/2$ and $3/2$ were examined [18,22]. It splits levels according to $J = N \pm S$, where S is the spin of the unpaired electron and couples states with $\Delta N = 0, \pm 1$ and $\Delta K_a = \pm 1$. Therefore, spin-rotation interaction destroys the goodness of both N and K_a quantum numbers. Its average matrix elements were found to be approximately 0.3 cm^{-1} [18].

(3) *Asymmetry*. NO_2 is not a symmetric top: the two large moments of inertia differ by approximately 4%. This asymmetry causes transitions between states with $\Delta K_a = 0, \pm 2$ [8]. However, this coupling is too weak to account for the effects observed in the spectra [13].

(4) *Hyperfine interaction* couples N and S to the nuclear spin, destroying J as a good quantum num-

ber. However, the matrix elements are small ($\approx$ 0.0025 cm^{-1}, Ref. [14]) and this coupling does not play a significant role.

Coriolis, centrifugal and spin-rotation interactions cause K_a-mixing below D_0 and this is presumed to also be the case above D_0. Actually, it can be argued that Coriolis and centrifugal interactions may be stronger above D_0 as a consequence of more pronounced large-amplitude motions. An important point is that the VR coupling time is finite above D_0 in the sense that the mixing process competes with dissociation. Thus, even if K_a is destroyed in the bound molecule, there are reasonable arguments for expecting less effective K_a-mixing above dissociation threshold.

3. Trajectory calculations

In this Letter, K_a-mixing in unimolecular dissociation is studied on the lowest *adiabatic* PES of NO_2. This PES has been calculated by ab initio methods and has mainly the character of the ground electronic state [23]. The focus is on Coriolis and centrifugal interactions. The nature of the PES and the classical trajectory method give no way of taking the spin–orbit interaction [18] into account. With just Coriolis and centrifugal interactions included, K_a-mixing is a direct measure of the VR interaction strength. An adiabatic description is plausible for NO_2 near the threshold. Note that the characteristic mixing time for the $^2A_1$ and $^2B_2$ states is $\approx$ 50 fs [15], which is two orders of magnitude shorter than the dissociation time. Calculation of the Lyapunov exponents has shown that one of the main features of the near-threshold vibrational dynamics, i.e. the strong irregularity [18], is reproduced with only the lowest PES taken into account.

The adiabatic three-dimensional (3D) PES describing both the inner and the asymptotic regions was calculated at the CASPT2 level using the natural orbitals obtained from CASSCF calculations. Details will be presented elsewhere [23]. The potential was slightly rescaled in order to reproduce the known experimental values for the fundamental transition frequencies and D_0. The PES has two minima, a deep global one, corresponding to the ground electronic state and a relatively shallow local minimum, $\approx$ 1.6 eV above the former. The local minimum is a result of the $^2B_2$ state. The two minima are separated by a small barrier, which reflects the conical intersection between the two electronic states. At the equilibrium geometry, the moments-of-inertia (in au) are $I_a^\circ = 12554 \ll I_b^\circ = 272850 \approx I_c^\circ = 285403$ and the a-axis passes through the midpoint of each NO bond. The energy associated with the transition $K_a = 0 \rightarrow K_a = 1$ is approximately 8 cm^{-1} for the equilibrium geometry. The potential along the O–NO interfragment distance is barrierless, and the zero-point energy of the NO fragment is 895 cm^{-1}. According to classical variational RRKM calculations, NO_2 vibrationally excited up to 100 cm^{-1} above threshold has a loose transition state at $\approx 6 a_0$ [23].

Numerical schemes for performing classical calculations including overall rotation are well developed [1] and initial conditions are usually imposed in the bound region [24]. In the present work, the initial conditions are imposed on the separated fragments and the reverse reaction is studied, i.e. recombination followed by subsequent dissociation (see, for example, Ref. [25]). This lessens the problem of non-conservation of the zero-point energy of the NO fragment, since the classical NO vibrational energy can be set at $0.5\hbar\omega_{NO}$. The central question, namely, to what extent is the phase space associated with K_a mixed, is not affected by this approach.

The calculations were carried out using the coordinate system proposed by Karplus et al. [26]. It consists of the Cartesian coordinates of the Jacobi vectors $\boldsymbol{R}$ (which connects the O atom with the center-of-mass of the NO fragment) and $\boldsymbol{r}$ (which connects the N and O atoms in the diatomic fragment) [27]. The total energy is approximated by:

$$E_{tot} = \epsilon_0 + B_0 N(N+1) + (A_0 - B_0) K_a^2, \qquad (1)$$

where ϵ_0 is the excess vibronic energy of the non-rotating molecule [10] and $A_0 = \hbar^2/2I_a^\circ$ and $B_0 = \hbar^2/2I_b^\circ$ are the equilibrium rotational constants. Initial conditions were selected as per Ref. [26]. The orientation of the diatom in space and its angular momentum were selected randomly and the impact parameter and fragment velocity in the center-of-mass system were adjusted to give the desired values of N and E_{tot}. The initial distance $|\boldsymbol{R}_0|$ was chosen to be

14 a_0 in all of the calculations; at this distance the interfragment potential is practically zero.

Dynamics are recorded once $|\boldsymbol{R}|$ drops below 7 a_0, which is about 1 a_0 larger than the RRKM transition state distance for the nonrotating molecule [23]. This region is the border between the inner part of the PES and the product space. In what follows, the 'clock' is set to zero when the system crosses this line. To define $K_a(t)$, the inertial tensor [28] is diagonalized at every integration step and the direction of the tensor axis a, corresponding to the lowest moment of inertia is found. Finally, $\boldsymbol{N}$ is projected onto the a-axis. The scheme for selecting the initial conditions creates a near-Gaussian distribution of initial values $K_a(0)$, which has a maximum at $K_a(0) = 0$. The number of trajectories calculated is sufficient to enable us to compare K_a-mixing for different values of $K_a(0)$. Trajectories are integrated until $|\boldsymbol{R}|$ or $|\boldsymbol{r}|$ passes the dividing line at 7 a_0. The time spent in the inner region of the potential is referred to as the lifetime τ.

There is no rigorous definition of the K_a-mixing degree for a single trajectory. Therefore, we use two figures-of-merit. The degree of K_a-mixing is obviously related to τ and therefore we define:

$$\Delta K_a^{(1)} = |\langle K_a \rangle - K_a(0)|, \tag{2}$$

where

$$\langle K_a \rangle = \frac{1}{\tau}\int_0^{\tau} K(t)\mathrm{d}t \tag{3}$$

is the average of $K_a(t)$ taken over the entire trajectory. This is a 'mild' criterion, as the (possible) sharp fluctuations in K_a are smoothed out. However, these fluctuations are used in the second figure-of-merit based on the maximum ($K_a^{\max}$) and minimum ($K_a^{\min}$) values of K_a along the trajectory:

$$\Delta K_a^{(2)} = K_a^{\max} - K_a^{\min}. \tag{4}$$

Eq. (4) gives the largest possible degree of K_a destruction. Note that while $\Delta K_a^{(1)}$ is bound by N, $\Delta K_a^{(2)}$ is bound by $2N$.

The excess vibronic energy ϵ_0 was chosen in the calculations to be approximately 15 cm^{-1}, which is close to the experimental conditions of Ref. [10] and calculations were performed for $N = 1,5,10,15$ and 20. A fifth-order Runge–Kutta integration scheme [29] with an initial time increment of 0.24 fs was used to solve the equations of motion. Energy and angular momentum were conserved to the 7th significant digit. For each N value, 20000 trajectories were calculated and analyzed.

4. Results

The first point to note is that almost all trajectories are strongly irregular. The Lyapunov exponents for 100 randomly selected trajectories were all found to be greater than 10 ps^{-1}, which indicates that randomization within the vibrational phase space occurs on a time scale of roughly 100 fs [30]. This irregularity is also reflected in the fluctuations of $K_a(t)$. It is significant that K_a rarely changes sign, which is probably a consequence of the fact that the rotational period is close to the dissociation time. As a result, the averaging in Eq. (3) does not contain significant cancellations of positive and negative contributions. Otherwise the definition of $\Delta K_a^{(1)}$ given in Eq. (2) would not be meaningful.

The average lifetime τ was found to be almost independent of N. For example, for $K_a(0) = 0$ the lifetime grows slightly with N, but the change is less than 10% over the range $1 \le N \le 20$. This is in qualitative agreement with the experimental rate constant, which was found to be almost independent of N [10]. However, since the present calculations are not suited for determining rate constants, this result could be fortuitous.

The extent of K_a-mixing based on Eq. (2) is presented in Figs. 1 and 2. Fig. 1 shows distributions of $\Delta K_a^{(1)}$ averaged over all trajectories, i.e. with the initial distributions of $K_a(0)$ values taken into account. The continuous ΔK_a scale was binned at half-integer and integer values. Two facts are apparent. First, every distribution peaks at $\Delta K_a^{(1)} = 0$. Second, the distributions become broader with N, indicating that VR coupling grows with N. Nonetheless, even for the largest angular momenta studied, modest $\Delta K_a^{(1)}$ values dominate. It was also found that the change of $K_a(t)$ along the trajectory does not depend much on the initial value $K_a(0)$. Therefore, in the subsequent discussion we select only trajectories with $K_a(0)$ near zero, which anyway

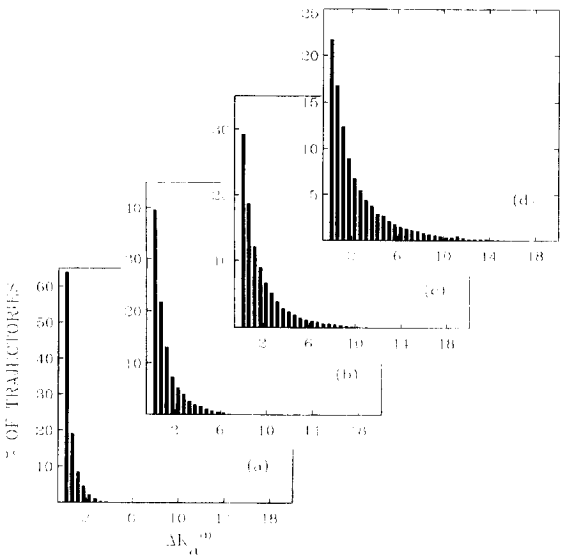

Fig. 1. Distributions of $\Delta K_a^{(1)}$, Eq. (2) for different values of the rotational angular momentum N: (a) $N = 5$; (b) $N = 10$; (c) $N = 15$; (d) $N = 20$.

have the largest weight in the distribution of initial values.

The extent of K_a-mixing is shown in Fig. 2, which gives percentages of trajectories with $\Delta K_a^{(1)} < 0.2N$ and $\Delta K_a^{(1)} > 0.4N$. For the former mixing is said to be weak, whereas for the latter mixing is said to be strong. Though subjective, these criteria provide a basis for classifying trajectories. More than 80% of the trajectories show weak mixing, whereas $< 10\%$ mix K_a strongly. These fractions are approximately independent of N. To rationalize this, recall that the Coriolis force and the volume of K_a space both increase roughly linearly with N. The former increases the degree of K_a-mixing, while the latter decreases it. Since the average lifetime in the calculations is almost independent of N, these effects act to cancel one another.

In addition to the VR coupling strength, the lifetime τ is the main quantity that determines the extent of K_a-mixing when the molecule dissociates. This is clearly demonstrated in Fig. 3 showing the fraction of K_a space which is mixed (f) vs. τ for all values of N considered (with $K_a(0) = 0$). The criteria given by Eqs. (2) and (4) are used to define $f^{(i)}(\tau)$:

$$f^{(1)}(\tau) = \Delta K_a^{(1)}/N, \tag{5}$$

$$f^{(2)}(\tau) = \Delta K_a^{(2)}/2N, \tag{6}$$

where the fact that $\Delta K_a^{(1)} \in (0,N)$ and $\Delta K_a^{(2)} \in (0,2N)$ has been used. The data points for $f^{(1)}(\tau)$ follow a single curve and the same holds true for the function $f^{(2)}(\tau)$. This reflects the independence of the mixing process from N. The 'dispersions' of the curves become significant only for long lifetimes, which is likely to be due to the insufficient number of long-lived trajectories (for example, only 50 trajectories out of 20000 contributed to the maximum $f^{(2)}(\tau)$ value for $N = 20$ in Fig. 3b). As expected, the figure-of-merit defined in Eq. (4) gives higher degrees of K_a-mixing, especially for smaller lifetimes. However, the difference between Eqs. (2) and (4) decreases with τ. In both cases, substantial mixing is observed only for trajectories living more than 8 ps and the full mixing, i.e. $f^{(i)} \approx 1$, is achieved only when τ exceeds 12 ps. It is worth mentioning, however, that the extremely small number of trajectories with large $\Delta K'$ values leaves the time of *complete* mixing poorly defined. For $\tau = 5$ ps, which is close to the experimental value [10], $f^{(1)} \approx 0.20$ and $f^{(2)} \approx 0.30$, i.e. 20%–30% of the K_a space is mixed.

Fig. 3 is the main result of the present work. It enables us to relate our observations to the conclusions drawn from the spectroscopic and time resolved experiments. In the former, the widths of the narrowest spectral features just a few cm^{-1} above

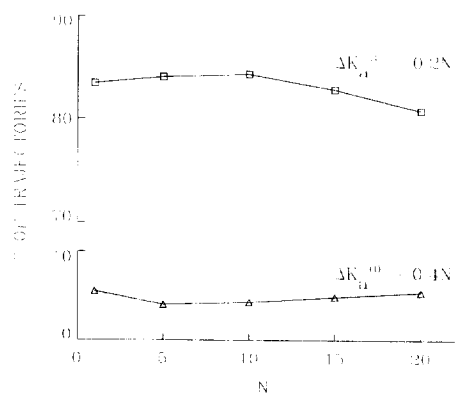

Fig. 2. The degree of K_a-mixing for trajectories with the initial value of $K_a(0) = 0$ as a function of the angular momentum N.

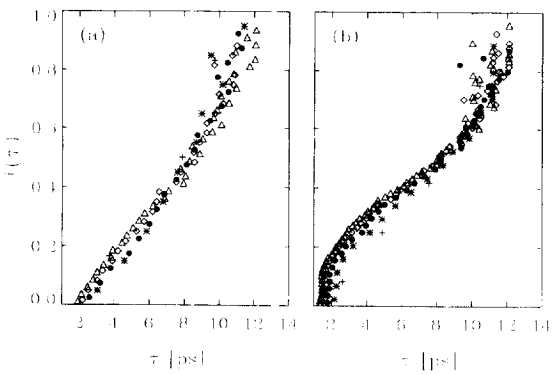

Fig. 3. The degree of K_a mixing $f(\tau)$, as a function of the trajectory lifetime: (a) $f^{(1)}(\tau)$, Eq. (5); (b) $f^{(2)}(\tau)$, Eq. (6). Different symbols refer to calculations with different rotational angular momentum N: (+) $N=1$; (*) $N=5$; (●) $N=10$; (◇) $N=15$; (△) $N=20$. Complete mixing corresponds to $f^{(i)}=1.0$. The lifetime τ is averaged over the trajectories 'falling' in a particular bin in ΔK_a. Because of ΔK_a binning, mixing cannot be discerned for $\tau < 2$ ps.

threshold were used to determine dissociation rates. The corresponding lifetimes range from about 10 to 50 ps. These resonances live long enough to allow complete mixing of the K_a space. This experiment is essentially 'blind' to processes with significantly shorter lifetimes, since broad widths blend into the background. However, the time-resolved experiments were carried out at slightly higher energies and buildup times ≈ 5 ps were recorded. For such timescales, K_a-mixing is predicted to be modest. Thus, there is no inconsistency: the difference reflects the different timescales to which the two experiments are sensitive.

Comparing the experimental conclusions regarding K_a-mixing with the results of the classical calculations on the basis of the $f^{(i)}(\tau)$ functions is more meaningful than comparing near-threshold dissociation rates. The former comparison does not suffer from the zero-point problem that plagues classical theories.

In summary, K_a-mixing brought about by Coriolis and centrifugal couplings in dissociating NO_2 has been examined. The central result is the observation of a direct relationship between the extent of mixing and the lifetime τ. Two different criteria used to obtain this relationship give consistent results. Though classical mechanics was used, we are confident that the result is also valid quantum mechanically. Fig. 3 is consistent with the experimental inferences: strong mixing in the spectroscopic experiments and weak mixing in the time-resolved experiments. However, another important mechanism of K_a-mixing – the spin–rotation interaction [18] – was not considered in the present work.

Acknowledgements

SYG acknowledges financial support from the Alexander von Humboldt Stiftung; he is also grateful to the Wittig group, especially I. Bezel and M. Dulligan, for their hospitality during his stay in Los Angeles, where this work was started. RS kindly acknowledges financial support by the Deutsche Forschungsgemeinschaft through the Sonderforschungsbereich 357 "Molekulare Mechanismen Unimolekularer Prozesse." The collaboration with the USC group was partly supported through a Max-Planck Forschungspreis.

References

[1] T. Baer, W.L. Hase, Unimolecular Reaction Dynamics, Oxford University Press, Oxford, 1996.
[2] R. Schinke, H.-M. Keller, H. Flöthmann, M. Stumpf, C. Beck, D.H. Mordaunt, A.J. Dobbyn, Adv. Chem. Phys. 101 (1997) 745.
[3] D.J. Nesbitt, R.W. Field, J. Phys. Chem. 100 (1996) 12735.
[4] A.J. Lichtenberg, M.A. Lieberman, Regular and Stochastic Motion, Springer-Verlag, New-York, 1983.
[5] T. Uzer, Phys. Rep. 199 (1991) 73.
[6] E.E. Aubanel, D.M. Wardlaw, L. Zhu, W.L. Hase, Int. Rev. Phys. Chem. 10 (1991) 249.
[7] J.H. Frederic, G.M. McClelland, P. Brumer, J. Chem. Phys. 83 (1985) 190.
[8] L.D. Landau, E.M. Lifshitz, Quantum Mechanics, Nonrelativistic Theory, Pergamon, New York, 1976.
[9] M. Quack, J. Troe, Ber. Bunsenges. Phys. Chem. 78 (1974) 240.
[10] P.I. Ionov, I. Bezel, S.I. Ionov, C. Wittig, Chem. Phys. Lett. 272 (1997) 257.
[11] J. Miyawaki, K. Yamanouchi, S. Tsuchiya, J. Chem. Phys. 99 (1993) 254.
[12] B. Abel, H.H. Hamann, V. Lange, Faraday Discuss. Chem. Soc. 102 (1995) 147.
[13] J.L. Hardwick, J. Mol. Spec. 109 (1985) 85.
[14] S.L. Coy, K.K. Lehmann, F.C. DeLucia, J. Chem. Phys. 85 (1986) 4297.

[5] K.K. Lehmann, S.L. Coy, Ber. Bunsenges. Phys. Chem. 92 (1988) 306.
[16] A. Delon, R. Jost, J. Chem. Phys. 95 (1991) 5686.
[17] A. Delon, R. Jost, M. Lombardi, J. Chem. Phys. 95 (1991) 5701.
[18] A. Delon, R. Georges, R. Jost, J. Chem. Phys. 103 (1995) 7740.
[19] S.A. Reid, H. Reisler, J. Chem. Phys. 101 (1994) 5683.
[20] S.I. Ionov, G.A. Bruckner, C. Jaques, Y. Chen, C. Wittig, J. Chem. Phys. 99 (1993) 3420.
[21] S.I. Ionov, H.F. Davis, K. Mikhaylichenko, L. Valachovic, R.A. Beaudet, C. Wittig, J. Chem. Phys. 101 (1994) 4809.
[22] A. Delon, P. Dupre, R. Jost, J. Chem. Phys. 99 (1991) 9482.
[23] S.Yu. Grebenshchikov, C. Beck, H. Flöthmann, R. Schinke, S. Kato, in preparation, 1997.
[24] G. Nyman, S. Nordholm, H.W. Schranz, J. Chem. Phys. 93 (1990) 6767.
[25] I.P. Hamilton, P. Brumer, J. Chem. Phys. 82 (1985) 595.
[26] M. Karplus, R.N. Porter, R.D. Sharma, J. Chem. Phys. 43 (1963) 3259.
[27] R. Schinke, Photodissociation Dynamics, Cambridge University Press, Cambridge, 1993.
[28] L.D. Landau, E.M. Lifshitz, Mechanics, Pergamon, New York, 1976.
[29] W.H. Press, S.A. Teukolsky, W.T. Vetterling, B.P. Flannery, Numerical Recipies in Fortran: the Art of Science Computing Cambridge University Press, Cambridge, 1992.
[30] G. Benettin, L. Galgani, J.M. Strelcyn, Phys. Rev. A 14 (1977) 2338.